

Extracting many-body correlators of saturated gluons with precision from inclusive photon+dijet final states in deeply inelastic scattering

Kaushik Roy^{1,2,*} and Raju Venugopalan^{2,†}

¹*Department of Physics and Astronomy, Stony Brook University, Stony Brook, NY 11794, USA*

²*Physics Department, Brookhaven National Laboratory, Bldg. 510A, Upton, NY 11973, USA*

(Dated: December 4, 2019)

We highlight the principal results of a computation [1] in the Color Glass Condensate effective field theory (CGC EFT) of the next-to-leading order (NLO) impact factor for inclusive photon+dijet production at Bjorken $x_{Bj} \ll 1$ in deeply inelastic electron-nucleus (e+A DIS) collisions. When combined with extant results for next-to-leading $\log x_{Bj}$ JIMWLK renormalization group (RG) evolution of gauge invariant two-point (“dipole”) and four-point (“quadrupole”) correlators of light-like Wilson lines, the inclusive photon+dijet e+A DIS cross-section can be determined to $\sim 10\%$ accuracy. Our computation simultaneously provides the ingredients to compute fully inclusive DIS, inclusive photon, inclusive dijet and inclusive photon+jet channels to the same accuracy. This makes feasible quantitative extraction of many-body correlators of saturated gluons and precise determination of the saturation scale $Q_{S,A}(x_{Bj})$ at a future Electron-Ion Collider. An interesting feature of our NLO result is the structure of the violation of the soft gluon theorem in the Regge limit. Another is the appearance in gluon emission of time-like non-global logs which also satisfy JIMWLK RG evolution.

The many-body recombination and screening of gluons in the high energy or small Bjorken x_{Bj} Regge limit of QCD competes with their rapid bremsstrahlung and leads to the perturbative unitarization of cross-sections. This gluon saturation phenomenon [2, 3], in the Color Glass Condensate (CGC) effective field theory (EFT) picture [4–10], occurs when the phase-space occupancy n of gluons for transverse momenta $k_{\perp} \leq Q_S(x_{Bj})$ becomes of the order of the inverse of the QCD coupling α_S . The saturation scale $Q_S(x_{Bj})$ is an emergent quantity and is the only large scale in the Regge limit; because it is much larger than intrinsic QCD scales, asymptotic freedom dictates that $\alpha_S(Q_S) \ll 1$. The large mode occupancy $n \sim 1/\alpha_S(Q_S) \gg 1$ therefore suggests that gluon saturation corresponds to a remarkable classicalization of QCD at high energies.

In this letter, we will discuss the first computation in the CGC EFT of the next-to-leading order (NLO) “impact factor” for inclusive photon+dijet production in deeply inelastic scattering of electrons off nuclei (e+A DIS) at high energies. A powerful motivation to perform the computation is the prospect of such measurements [11] at a future Electron-Ion Collider (EIC) [12, 13]. As we will outline here, knowing the NLO impact factor will enable us to compute the photon+dijet cross-section in e+A DIS to $O(\alpha_S^3 \ln(1/x_{Bj}))$ accuracy. The details of the computation are spelled out in a companion paper [1]. At the energies and nuclear saturation scales accessible at an EIC, the computations allow predictions to $\sim 10\%$ accuracy [14]. This may be sufficient for precision tests of the CGC EFT and to distinguish its predictions from those of potential alternative frameworks.

It is instructive to first briefly consider our previous computation [15] in the CGC EFT of the leading order

(LO) inclusive photon+dijet ($\gamma + q\bar{q}$) e+A DIS cross-section:

$$\frac{d^3\sigma^{\text{LO};\gamma+q\bar{q}+X}}{dx dQ^2 d^6K_{\perp} d^3\eta_K} = \frac{\alpha_{em}^2 q_f^4 y^2 N_c}{512\pi^5 Q^2} \frac{1}{(2\pi)^4} \frac{1}{2} L^{\mu\nu} \tilde{X}_{\mu\nu}^{\text{LO}}. \quad (1)$$

Here $\alpha_{em} = e^2/4\pi$ is the electromagnetic fine structure constant, $y = q \cdot P_N / \tilde{l} \cdot P_N$ is the inelasticity, $Q^2 = -q^2 > 0$ is the squared momentum transfer from the nucleus, and $d^6K_{\perp} d^3\eta_K$ collectively denotes the phase space density of final state quark, anti-quark and photon. Likewise, $L^{\mu\nu}$ is the lepton tensor, corresponding to the emission of a virtual photon with four momentum q^{μ} by the electron [16]. Our focus here is on the scattering of the virtual photon on the nuclear target producing the $\gamma + q\bar{q}$ final state and other (phase space integrated) X particles, described by the LO hadron tensor,

$$\tilde{X}_{\mu\nu}^{\text{LO}} = \int [\mathcal{D}\rho_A] W_{\Lambda_0^-}[\rho_A] \hat{X}_{\mu\nu}^{\text{LO}}[\rho_A]. \quad (2)$$

In a Born-Oppenheimer separation of modes in the EFT, the ρ_A are the large x_{Bj} static color sources in the nucleus; these correspond to light cone longitudinal momentum modes with $\Lambda^- < \Lambda_0^-$. The initial distribution of such modes at the scale Λ_0^- is given by the non-perturbative gauge invariant weight functional $W_{\Lambda_0^-}[\rho_A]$. The small x_{Bj} dynamical gluon fields interacting with the probe correspondingly have longitudinal momenta above Λ_0^- ; the leading order classical gluon field is a “shock wave” solution of the Yang-Mills (YM) equations in the presence of the sources $\rho^a(\mathbf{x}) = \tilde{\rho}^a(\mathbf{x}_{\perp})\delta(x^-)$ [17] of $O(1/g)$.

The solution of the YM equations in the Lorenz gauge $\partial_{\mu}A^{\mu} = 0$ (or equivalently light cone (LC) $A^- = 0$ gauge)

is given by

$$\begin{aligned} A_{\text{cl}}^+ &= \int \frac{d^2 \mathbf{z}_\perp}{4\pi} \ln \frac{1}{(\mathbf{x}_\perp - \mathbf{z}_\perp)^2 \Lambda^2} \rho_A(x^-, \mathbf{z}_\perp), \\ A_{\text{cl}}^- &= 0; \quad A_{\text{cl},\perp} = 0, \end{aligned} \quad (3)$$

where Λ is an infrared cutoff necessary to invert the Laplace equation $-\nabla_\perp^2 A_{\text{cl}}^+ = g\rho_A$. This solution in Lorenz gauge is simply related to the solution in the LC gauge $A^+ = 0$, with $A_{\text{cl}}^- = 0$ and $\tilde{A}_{\text{cl}}^i = \frac{i}{g} U \partial^i U^\dagger$, where the adjoint lightlike Wilson line

$$U(\mathbf{x}_\perp) = P_- \left(\exp \left\{ -ig \int_{-\infty}^{+\infty} dz^- A_{\text{cl}}^{+,a}(z^-, \mathbf{x}_\perp) T^a \right\} \right). \quad (4)$$

is expressed in terms of the the large x static color source densities via Eq. 3. Note that T^a , $a = 1, \dots, 8$, are the generators of color $SU(3)$ in the adjoint representation. This x^- path ordered exponential, and its fundamental representation counterpart $\tilde{U}(\mathbf{x}_\perp)$ (obtained by replacing T^a with the Gell-Mann matrices t^a), efficiently resum all higher twist contributions $\frac{\rho_A}{\Lambda^2} \rightarrow \frac{Q_s}{Q^2}$ from the multiple scattering of the $q\bar{q}$ pair off the color field of the nucleus.

The LO $\gamma + q\bar{q}$ amplitude is obtained by solving the Dirac equation in the A_{cl}^+ shock wave background in the $A^- = 0$ LC gauge. A Feynman diagram for the LO process is shown in Fig. 1, where the vertical dashed line represents the cut separating the amplitude from its complex conjugate amplitude and the horizontal dashed line separates the dynamical projectile modes from the static target shock wave gauge fields at the scale Λ_0^- . The dressed shock wave propagator, denoted by cross-hatch circles in the figure, has the remarkably simple solution [6, 18],

$$S_{ij}(p, q) = S_0(p) \mathcal{T}_{q;ij}(p, q) S_0(q), \quad (5)$$

where $S_0(p) = \frac{i\not{p}}{p^2 + i\epsilon}$ is the free massless fermion propagator, and

$$\begin{aligned} \mathcal{T}_{q;ji}(q, p) &= 2\pi \delta(p^- - q^-) \gamma^- \text{sign}(q^-) \\ &\times \int d^2 \mathbf{z}_\perp e^{-i(\mathbf{q}_\perp - \mathbf{p}_\perp) \cdot \mathbf{z}_\perp} \tilde{U}_{ji}^{\text{sign}(q^-)}(\mathbf{z}_\perp), \end{aligned} \quad (6)$$

is the effective vertex corresponding to the multiple scattering of the quark or antiquark off the shock wave [19]. The LO computation of the $\gamma + q\bar{q}$ cross-section in $A^- = 0$ gauge is straightforward and one finds,

$$\begin{aligned} \tilde{X}_{\mu\nu}^{\text{LO}} &= 2\pi \delta(1 - z_q - z_{\bar{q}} - z_\gamma) \int d\Pi_\perp^{\text{LO}} \int d\Pi_\perp^{\text{LO}*} \tau_{\mu\nu}^{q\bar{q}, q\bar{q}}(\mathbf{l}_\perp, \mathbf{l}'_\perp) \\ &\times \Xi(\mathbf{x}_\perp, \mathbf{y}_\perp; \mathbf{y}'_\perp, \mathbf{x}'_\perp), \end{aligned} \quad (7)$$

where we introduced the compact notation [20],

$$\int d\Pi_\perp^{\text{LO}} = \int_{\mathbf{l}_\perp} \int_{\mathbf{x}_\perp, \mathbf{y}_\perp} e^{i\mathbf{l}_\perp \cdot (\mathbf{x}_\perp - \mathbf{y}_\perp) - i(\mathbf{k}_\perp + \mathbf{k}_{\gamma\perp}) \cdot \mathbf{x}_\perp - i\mathbf{p}_\perp \cdot \mathbf{y}_\perp}. \quad (8)$$

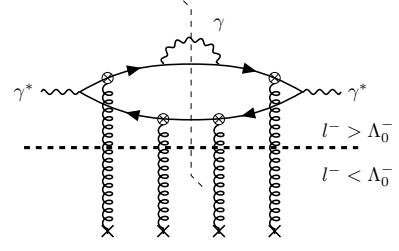


FIG. 1. A representative LO diagram. The cross-hatched open blobs represent the dressed quark propagator in $A^- = 0$ gauge. See text for details.

The function $\tau_{\mu\nu}^{q\bar{q}, q\bar{q}}(\mathbf{l}_\perp, \mathbf{l}'_\perp)$ denotes the spinor trace in the LO cross-section [15].

The nonperturbative input from the dynamics of saturated gluons in the nuclear target is contained in

$$\Xi(\mathbf{x}_\perp, \mathbf{y}_\perp; \mathbf{y}'_\perp, \mathbf{x}'_\perp) = 1 - D_{xy} - D_{y'x'} + Q_{y'x';xy}. \quad (9)$$

Here

$$\begin{aligned} D_{xy} &= \frac{1}{N_c} \left\langle \text{Tr} \left(\tilde{U}(\mathbf{x}_\perp) \tilde{U}^\dagger(\mathbf{y}_\perp) \right) \right\rangle, \\ Q_{xy;zw} &= \frac{1}{N_c} \left\langle \text{Tr} \left(\tilde{U}(\mathbf{x}_\perp) \tilde{U}^\dagger(\mathbf{y}_\perp) \tilde{U}(\mathbf{z}_\perp) \tilde{U}^\dagger(\mathbf{w}_\perp) \right) \right\rangle, \end{aligned} \quad (10)$$

represent respectively the dipole and quadrupole Wilson line correlators, where

$$\langle \hat{\mathcal{O}} \rangle = \int [\mathcal{D}\rho_A] W_{\Lambda_0^-}[\rho_A] \hat{\mathcal{O}}[\rho_A], \quad (11)$$

denotes the expectation value of a generic operator $\hat{\mathcal{O}}$. The weight functional $W_{\Lambda_0^-}[\rho_A]$ contains fundamental information about n -body correlations amongst the color sources at the scale Λ_0^- . In the McLerran-Venugopalan model (MV) [4–6] where it was introduced, $W_{\Lambda_0^-}[\rho_A]$ is Gaussian distributed for a large nucleus [5, 21, 22] with a variance $\mu_A^2 \sim A^{1/3}$, where A denotes the atomic number. In the MV model, $\mu_A^2 \propto Q_{S,0}^2$, the saturation scale at Λ_0^- [7, 23]. For quantitative estimates of the saturation scale at EIC energies, we refer the reader to [13, 24]. In the CGC EFT, D and Q appear in a variety of LO processes in both $p + A$ and $e + A$ collisions [25].

We turn now to the extension of our computation of $\tilde{X}_{\mu\nu}$ to NLO, details of which are provided in [1]. Let us first consider the NLO diagram in Fig. 2. An important ingredient in our computation is the gluon “small fluctuations” propagator in the $A^- = 0$ gauge classical shock wave background field [6, 15, 26–28]:

$$G_{\mu\rho;ab}(p, q) = G_{\mu\rho;ac}^0(p) \mathcal{T}_g^{\rho\sigma;cd}(p, q) G_{\sigma\nu;db}^0(q), \quad (12)$$

where $G_{\mu\rho;ac}^0(p) = \frac{i}{p^2 + i\epsilon} \left(-g_{\mu\rho} + \frac{p_\mu n_\rho + n_\mu p_\rho}{n \cdot p} \right) \delta_{ac}$ is the free propagator with Lorentz indices μ, ρ , color indices

a, c and $n^\mu = \delta^{\mu+}$. The effective gluon vertex

$$\begin{aligned} \mathcal{T}_g^{\mu\nu;ab}(p, p') &= -2\pi\delta(p^- - p'^-) \times (2p^-)g^{\mu\nu} \text{sign}(p^-) \\ &\times \int d^2z_\perp e^{-i(\mathbf{p}_\perp - \mathbf{p}'_\perp) \cdot \mathbf{z}_\perp} \left(U^{ab} \right)^{\text{sign}(p^-)}(\mathbf{z}_\perp), \end{aligned} \quad (13)$$

corresponding to multiple scattering of the gluon off the shock wave background field, is represented by the filled blobs in Fig. 2.

In the NLO diagrams represented in Fig. 2, the contributions enhanced by $\alpha_S \ln(\Lambda_1^-/\Lambda_0^-)$ (with Λ_1^- chosen such that these terms are $O(1)$) can be combined with the LO result in Eq. (2) and expressed as [29],

$$\begin{aligned} \tilde{X}_{\mu\nu}^{\text{LO}} + \delta\tilde{X}_{\mu\nu}^{\text{NLO}:1} &= \int [\mathcal{D}\rho_A] \left(1 + \ln(\Lambda_1^-/\Lambda_0^-) \mathcal{H}_{\text{LO}} \right) W_{\Lambda_0^-}[\rho_A] \\ &\times \hat{X}_{\mu\nu}^{\text{LO}}[\rho_A]. \end{aligned} \quad (14)$$

Further redefining

$$\left(1 + \ln(\Lambda_1^-/\Lambda_0^-) \mathcal{H}_{\text{LO}} \right) W_{\Lambda_0^-}[\rho_A] = W_{\Lambda_1^-}[\rho_A], \quad (15)$$

and thereby absorbing the semi-fast gluon fluctuations of the target in a modification of the weight functional of the color sources at the scale Λ_1^- , one obtains the leading log in x (LL x) [30] JIMWLK renormalization group equation [31],

$$\frac{\partial}{\partial(\ln \Lambda^-)} W_{\Lambda^-}[\rho_A] = \mathcal{H}_{\text{LO}} W_{\Lambda^-}[\rho_A], \quad (16)$$

where \mathcal{H}_{LO} is the well-known JIMWLK Hamiltonian [32–35]. We will henceforth label the weight functional that satisfies Eq. (16) as $W^{LLx}[\rho_A]$.

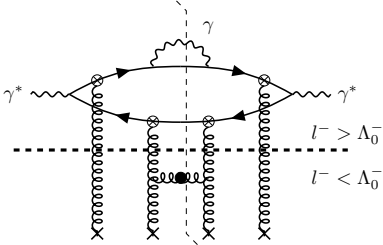


FIG. 2. NLO leading logs in x ($\alpha_S \ln(1/x) \sim 1$) diagram with the same $O(1)$ contributions as the LO diagram in Fig. 1. The filled blob represents the dressed gluon propagator in $A^- = 0$ gauge. See text for details.

At next-to-next-to-leading order (NNLO) in α_S , there are two relevant classes of contributions as illustrated in Fig. 3. Diagrams corresponding to a two loop fluctuation of the target are shown in Fig. 3(a). For such two loop diagrams, contributions of order $\alpha_S^2 \ln^2(\Lambda_1^-/\Lambda_0^-) \sim O(1)$ are included in $W^{LLx}[\rho_A]$. We will therefore consider here only the two loop diagrams that contain next-to-leading logarithms in x (NLL x) contributions to

Eq. 14. The LO+NLL x result including these can be expressed as

$$\tilde{X}_{\mu\nu}^{\text{LO}} + \delta\tilde{X}_{\mu\nu}^{\text{NLL}x} = \int [\mathcal{D}\rho_A] W_{\Lambda_1^-}^{\text{NLL}x}[\rho_A] \hat{X}_{\mu\nu}^{\text{LO}}[\rho_A], \quad (17)$$

where

$$W_{\Lambda_1^-}^{\text{NLL}x}[\rho_A] = \left\{ 1 + \ln(\Lambda_1^-/\Lambda_0^-) (\mathcal{H}_{\text{LO}} + \mathcal{H}_{\text{NLO}}) \right\} W_{\Lambda_0^-}[\rho_A], \quad (18)$$

and the NLO JIMWLK Hamiltonian \mathcal{H}_{NLO} computed in [37–41] (see also [42, 43]) is of order α_S^2 .

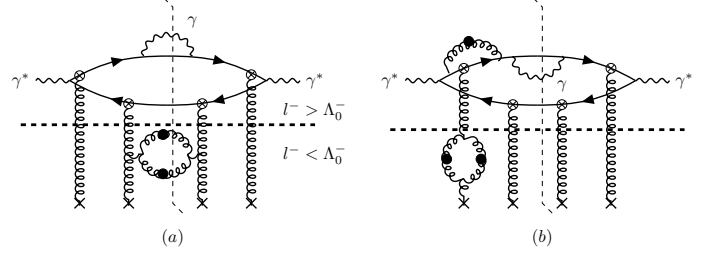


FIG. 3. (a) NNLO diagram corresponding to target fluctuations of $O(\alpha_S^2 \ln(1/x))$. Such contributions are resummed to all orders by the NLO JIMWLK equation. (b) NNLO diagram with $O(\alpha_S \ln(1/x))$ fluctuations of the target and $O(\alpha_S)$ fluctuations of the projectile. These projectile fluctuations constitute the NLO γ +dijet impact factor.

The second class of NNLO contributions (formally of $O(\alpha_S^2)$), shown in Fig. 3(b), correspond to one loop fluctuations of both the projectile and the target. Specifically, the $\alpha_S \ln(1/x)$ contributions from the gluon fluctuations below the cut Λ_0^- are matched to the finite contributions above the cut (without logarithms) of $O(\alpha_S)$ in the real and virtual corrections to the LO photon+dijet projectile final state. These finite terms constitute the NLO γ +dijet impact factor. Together, they give for the class of NNLO contributions in Fig. 3(b),

$$\tilde{X}_{\mu\nu}^{\text{NNLO};\text{finite}} = \int [\mathcal{D}\rho_A] W^{LLx}[\rho_A] \hat{X}_{\mu\nu}^{\text{NNLO};\text{finite}}[\rho_A]. \quad (19)$$

Combining the expressions in Eqs. 17 and 19, the hadron tensor for inclusive photon+dijet production to NLO+NLL x accuracy can be written as

$$\begin{aligned} \tilde{X}_{\mu\nu}^{\text{NLO+NLL}x} &= \int [\mathcal{D}\rho_A] \left\{ W^{NLLx}[\rho_A] \hat{X}_{\mu\nu}^{\text{LO}}[\rho_A] \right. \\ &+ \left. W^{LLx}[\rho_A] \hat{X}_{\mu\nu}^{\text{NNLO};\text{finite}}[\rho_A] \right\} \\ &\simeq \int [\mathcal{D}\rho_A] \left(W^{NLLx}[\rho_A] \left\{ \hat{X}_{\mu\nu}^{\text{LO}}[\rho_A] + \hat{X}_{\mu\nu}^{\text{NNLO};\text{finite}}[\rho_A] \right\} \right. \\ &+ \left. O(\alpha_S^3 \ln(\Lambda_1^-/\Lambda_0^-)) \right). \end{aligned} \quad (20)$$

Our knowledge of the NLO impact factor and NLL x JIMWLK evolution can be combined, as shown above and in Fig. 4, to extend the scope of the computation to

$O(\alpha_S^3 \ln(1/x))$. However as the \simeq symbol indicates, this knowledge is insufficient to capture all the diagrams that contribute to this accuracy.

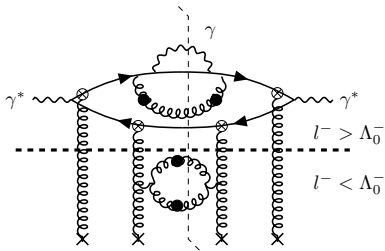


FIG. 4. N³LO diagrams including $O(\alpha_S)$ fluctuations of the projectile and $O(\alpha_S^2 \ln(1/x))$ fluctuations of the target. Such contributions can be computed using extant results for NLO JIMWLK and the NLO impact factor computed in [1].

We shall now sketch the key features of the computation of the inclusive NLO photon+dijet impact factor in [1]. The quantum fluctuations (with $l^- > \Lambda_0^-$) that contribute towards the NLO impact factor can be broadly classified into the modulus squared of real gluon emission amplitudes and the interference of virtual gluon exchange processes with LO diagrams. In each case, the real or virtual gluon can scatter off the shock wave or propagate freely without scattering; in addition, there are all possible permutations of the emission vertex of the final state photon. For real emissions alone, there are 400 possible diagrams – see [1] for the complete set of real and virtual graphs contributing at NLO. These can be categorized systematically by their color structures, allowing one to clearly observe the cancellation of the soft, collinear and ultraviolet (UV) divergences that arise in the intermediate steps of our computation.

Soft singularities arise from the spurious $l^- = 0$ pole in the free gluon propagator in $A^- = 0$ LC gauge. These are regulated by imposing a cutoff at the initial scale of evolution Λ_0^- . We show in [1] that log divergent terms in Λ_0^- in the “slow” gluon $l^- \rightarrow 0$ limit possess color structures at NLO identical to those resulting from the action (as shown in [44]) of the JIMWLK kernel on Ξ in Eq. 9. Our computation therefore provides an explicit proof of high energy JIMWLK factorization for a non-trivial process other than fully inclusive DIS.

The UV divergences are extracted using dimensional

regularization in $d = 2 - \epsilon$ dimensions. For gluon loops, most of the UV divergences cancel between graphs at the amplitude level. There are however residual collinear divergences. Such collinear singularities also arise from real gluon emission when integrating over the phase space in which the gluon can be collinear to the quark or antiquark. Because we are not integrating over the momenta of our $\gamma + q\bar{q}$ final state, there are collinear divergences that survive the real-virtual cancellations. These can be absorbed into a jet algorithm. Infrared (IR) safe quantities are obtained by promoting the partons to jets and working in the small cone approximation [45] of jet cone radius $R \ll 1$. This restricts the integration over the phase space for the real gluon. The dominant contribution is of the form $\alpha_S(A \ln(R) + B)$, where A, B , spelled out in [1], are of $O(1)$; all non-collinearly divergent contributions are phase space suppressed by powers of R^2 .

The jet algorithm also allows for a cancellation of soft-collinear divergences between soft gluon emissions inside and outside the jet cone. In the latter case, we observe that slow gluon emissions at wide angles ($l^- \rightarrow 0$ but any l_\perp), satisfy JIMWLK evolution and must be subtracted from the jet cross-section to avoid double counting when the NLO impact factor is combined with small x evolution [46]. This result is an explicit realization of the conformal spacelike-timelike correspondence noted previously by Mueller [47].

We also observe interestingly that, as a consequence of the different topologies of the color structures that contribute towards soft and collinear divergences, the soft gluon theorem is violated for inclusive photon+dijet production [48]. The factorization violating term has the color structure $(Q - DD)$. Since the building block of Q and D is the x^- path ordered Wilson line in Eq. 4, it would be interesting to explore if the soft gluon theorem can be restored by modifying the boundary conditions of the quadrupole and dipole operators at $x^- = \pm\infty$ [49].

After due consideration of all divergences, our final result for the triple differential cross-section for the $\gamma + q\bar{q}$ jet production in e+A DIS is

$$\frac{d^3\sigma^{\text{LO+NLO+NLL}x;\text{jet}}}{dx dQ^2 d^6K_\perp d^3\eta_K} = \frac{\alpha_{em}^2 q_f^4 y^2 N_c}{512\pi^5 Q^2} \frac{1}{(2\pi)^4} \frac{1}{2} \times L^{\mu\nu} \tilde{X}_{\mu\nu}^{\text{NLO+NLL}x;\text{jet}}, \quad (21)$$

where the hadron tensor at $O(\alpha_S^3 \ln(1/x))$ accuracy can be written as

$$\tilde{X}_{\mu\nu}^{\text{NLO+NLL}x;\text{jet}} = \int [D\rho_A] W_{x_{\text{Bj}}}^{\text{NLL}x}[\rho_A] \left[\left(1 + \frac{2\alpha_S C_F}{\pi} \left\{ -\frac{3}{4} \ln \left(\frac{R^2 |\mathbf{p}_{J\perp}| |\mathbf{p}_{K\perp}|}{4z_J z_K Q^2 e^{\gamma_E}} \right) + \frac{7}{4} - \frac{\pi^2}{6} \right\} \right) \tilde{X}_{\mu\nu}^{\text{LO};\text{jet}}[\rho_A] + \tilde{X}_{\mu\nu;\text{finite}}^{\text{NLO};\text{jet}}[\rho_A] \right]. \quad (22)$$

In this expression [50], the finite terms $\tilde{X}_{\mu\nu;\text{finite}}^{\text{NLO};\text{jet}}$ are of order α_S relative to the leading term and constitute the NLO impact factor. The explicit results for these are the principal results of [1]. For the virtual gluon diagrams, where the isolation of divergent and finite pieces is done at the amplitude level, it is straightforward albeit tedious to derive analytical expressions for such terms. This is however not possible for real gluon emission graphs; we need to evaluate the finite pieces numerically. These are obtained by taking the modulus squared of the real emission amplitudes, integrating over the gluon phase space with a cutoff, implementing the jet algorithm, and subsequently subtracting the pieces that contribute to leading log JIMWLK evolution.

The numerical computation of the finite pieces constituting $\tilde{X}_{\mu\nu;\text{finite}}^{\text{NLO};\text{jet}}$, along with NLO BK/JIMWLK evolution, provide the necessary ingredients to compute photon+dijet production (and associated measurement channels) in e+A DIS to $O(\alpha_S^3 \ln(1/x))$ accuracy. Prior NLO studies on DIS at small x focused on the cross-section for fully inclusive DIS [51–59], a noteworthy exception being the NLO studies of diffractive dijet and exclusive vector meson production by Boussarie et al. [60–62]. In this regard, our work goes a step beyond by considering more differential final states. The realization of these precision studies, while a formidable task, is feasible and will pave the way towards the quantitative global analyses of data required to uncover definitive evidence of gluon saturation.

We note finally that the simple forms of the momentum space shockwave propagators in $A^- = 0$ gauge and the momentum space techniques employed in our work [1, 15] will allow us to extend the accuracy of our computation to two loops. It is also worth mentioning that our NLO real gluon emission computation contains the LO results for the production cross-sections for 4-jet $\gamma + q\bar{q}g$ and 3-jet $q\bar{q}g$ [63] final states at small x . One may also consider employing this framework in p+A collisions, beyond the current state-of-the art for inclusive hadron [64–68], quarkonium [69, 70] and photon production [71–73], to NNLO in the CGC power counting and beyond.

This material is based on work supported by the U.S. Department of Energy, Office of Science, Office of Nuclear Physics, under Contracts No. de-sc0012704 and within the framework of the TMD Theory Topical Collaboration. K. R is supported by an LDRD grant from Brookhaven Science Associates and by the Joint BNL-Stony Brook Center for Frontiers in Nuclear Science (CFNS).

* kaushik.roy.1@stonybrook.edu

† ra.ju@bnl.gov

[1] Kaushik Roy and Raju Venugopalan, “NLO impact fac-

tor for inclusive photon+dijet production in $e + A$ DIS at small x ,” (2019), arXiv:1911.04530 [hep-ph].

- [2] L. V. Gribov, E. M. Levin, and M. G. Ryskin, “Semihard Processes in QCD,” *Phys. Rept.* **100**, 1–150 (1983).
- [3] Alfred H. Mueller and Jian-wei Qiu, “Gluon Recombination and Shadowing at Small Values of x ,” *Nucl. Phys.* **B268**, 427–452 (1986).
- [4] Larry D. McLerran and Raju Venugopalan, “Computing quark and gluon distribution functions for very large nuclei,” *Phys. Rev.* **D49**, 2233–2241 (1994), arXiv:hep-ph/9309289 [hep-ph].
- [5] Larry D. McLerran and Raju Venugopalan, “Gluon distribution functions for very large nuclei at small transverse momentum,” *Phys. Rev.* **D49**, 3352–3355 (1994), arXiv:hep-ph/9311205 [hep-ph].
- [6] Larry D. McLerran and Raju Venugopalan, “Green’s functions in the color field of a large nucleus,” *Phys. Rev.* **D50**, 2225–2233 (1994), arXiv:hep-ph/9402335 [hep-ph].
- [7] Edmond Iancu and Raju Venugopalan, “The Color glass condensate and high-energy scattering in QCD,” in *In *Hwa, R.C. (ed.) et al.: Quark gluon plasma* 249-3363* (2003) arXiv:hep-ph/0303204 [hep-ph].
- [8] Francois Gelis, Edmond Iancu, Jamal Jalilian-Marian, and Raju Venugopalan, “The Color Glass Condensate,” *Ann. Rev. Nucl. Part. Sci.* **60**, 463–489 (2010), arXiv:1002.0333 [hep-ph].
- [9] Yuri V. Kovchegov and Eugene Levin, *Quantum chromodynamics at high energy*, Vol. 33 (Cambridge University Press, 2012).
- [10] Jean-Paul Blaizot, “High gluon densities in heavy ion collisions,” *Rept. Prog. Phys.* **80**, 032301 (2017), arXiv:1607.04448 [hep-ph].
- [11] Our highly differential computation will allow us to provide, to the same accuracy, cross-sections for inclusive dijet, inclusive photon, inclusive photon and fully inclusive DIS measurements.
- [12] A. Accardi *et al.*, “Electron Ion Collider: The Next QCD Frontier,” *Eur. Phys. J.* **A52**, 268 (2016), arXiv:1212.1701 [nucl-ex].
- [13] E. C. Aschenauer, S. Fazio, J. H. Lee, H. Mantysaari, B. S. Page, B. Schenke, T. Ullrich, R. Venugopalan, and P. Zurita, “The Electron-Ion Collider: Assessing the Energy Dependence of Key Measurements,” (2017), arXiv:1708.01527 [nucl-ex].
- [14] An important caveat is that this statement is modulo the scale and scheme dependence of the results, which remain to be quantified.
- [15] Kaushik Roy and Raju Venugopalan, “Inclusive prompt photon production in electron-nucleus scattering at small x ,” *JHEP* **05**, 013 (2018), arXiv:1802.09550 [hep-ph].
- [16] Explicit expressions for all kinematic variables are provided in [15] and in [1].
- [17] The delta function corresponds to the Lorentz contraction of the sources in a frame where the momentum of the right moving nucleus, $P_N^+ \rightarrow \infty$.
- [18] Larry D. McLerran and Raju Venugopalan, “Fock space distributions, structure functions, higher twists and small x ,” *Phys. Rev.* **D59**, 094002 (1999), arXiv:hep-ph/9809427 [hep-ph].
- [19] The $\mathbf{1}$ term in the expansion of the Wilson lines corresponds to the possibility that either the quark or the antiquark does not scatter. Since at least one of them must, one should subtract a term from the net amplitude wherein \tilde{U} (and U) are set to unity everywhere.

- [20] The second such term appearing in Eq. 7 results from the complex conjugate of Eq. 8 and corresponds to replacing all transverse coordinates and internal momenta therein by their primed counterparts.
- [21] Yuri V. Kovchegov, “NonAbelian Weizsacker-Williams field and a two-dimensional effective color charge density for a very large nucleus,” *Phys. Rev.* **D54**, 5463–5469 (1996), arXiv:hep-ph/9605446 [hep-ph].
- [22] Sangyong Jeon and Raju Venugopalan, “Random walks of partons in $SU(N(c))$ and classical representations of color charges in QCD at small x ,” *Phys. Rev.* **D70**, 105012 (2004), arXiv:hep-ph/0406169 [hep-ph].
- [23] T. Lappi, “Wilson line correlator in the MV model: Relating the glasma to deep inelastic scattering,” *Eur. Phys. J.* **C55**, 285–292 (2008), arXiv:0711.3039 [hep-ph].
- [24] H. Kowalski, T. Lappi, and R. Venugopalan, “Nuclear enhancement of universal dynamics of high parton densities,” *Phys. Rev. Lett.* **100**, 022303 (2008), arXiv:0705.3047 [hep-ph].
- [25] Group theory techniques to compute such correlators in the MV model are discussed in [74–77].
- [26] Alejandro Ayala, Jamal Jalilian-Marian, Larry D. McLerran, and Raju Venugopalan, “Quantum corrections to the Weizsacker-Williams gluon distribution function at small x ,” *Phys. Rev.* **D53**, 458–475 (1996), arXiv:hep-ph/9508302 [hep-ph].
- [27] Alejandro Ayala, Jamal Jalilian-Marian, Larry D. McLerran, and Raju Venugopalan, “The Gluon propagator in nonAbelian Weizsacker-Williams fields,” *Phys. Rev.* **D52**, 2935–2943 (1995), arXiv:hep-ph/9501324 [hep-ph].
- [28] I. I. Balitsky and Andrei V. Belitsky, “Nonlinear evolution in high density QCD,” *Nucl. Phys.* **B629**, 290–322 (2002), arXiv:hep-ph/01110158 [hep-ph].
- [29] We employ here the Hermiticity of W with respect to the functional integration over ρ_A .
- [30] The LC momentum fraction x is equated to the Bjorken variable x_{Bj} here. The precise relation between the two is established beyond this order of the computation.
- [31] To LL x , this equation generates the Balitsky hierarchy [78] describing the evolution of n -point Wilson line correlators in x . In the limit of large number of colors N_c , and for $A \gg 1$, the simplest dipole correlator of light-like Wilson lines in this hierarchy satisfies the Balitsky-Kovchegov (BK) equation [78, 79]. In the leading twist limit where $Q_S^2(x)/Q^2 \ll 1$, it reduces to the BFKL equation [80, 81].
- [32] Jamal Jalilian-Marian, Alex Kovner, Andrei Leonidov, and Heribert Weigert, “The Wilson renormalization group for low x physics: Towards the high density regime,” *Phys. Rev.* **D59**, 014014 (1998), arXiv:hep-ph/9706377 [hep-ph].
- [33] Jamal Jalilian-Marian, Alex Kovner, and Heribert Weigert, “The Wilson renormalization group for low x physics: Gluon evolution at finite parton density,” *Phys. Rev.* **D59**, 014015 (1998), arXiv:hep-ph/9709432 [hep-ph].
- [34] Edmond Iancu, Andrei Leonidov, and Larry D. McLerran, “Nonlinear gluon evolution in the color glass condensate. 1.” *Nucl. Phys.* **A692**, 583–645 (2001), arXiv:hep-ph/0011241 [hep-ph].
- [35] Elena FERREIRO, Edmond Iancu, Andrei Leonidov, and Larry McLerran, “Nonlinear gluon evolution in the color glass condensate. 2.” *Nucl. Phys.* **A703**, 489–538 (2002), arXiv:hep-ph/0109115 [hep-ph].
- [36] There are also contributions from two-loop QCD diagrams proportional to α_S^2 alone (without leading logs in x) but these are suppressed at the desired accuracy of our problem.
- [37] Ian Balitsky and Giovanni A. Chirilli, “Rapidity evolution of Wilson lines at the next-to-leading order,” *Phys. Rev.* **D88**, 111501 (2013), arXiv:1309.7644 [hep-ph].
- [38] Alex Kovner, Michael Lublinsky, and Yair Mulian, “Jalilian-Marian, Iancu, McLerran, Weigert, Leonidov, Kovner evolution at next to leading order,” *Phys. Rev.* **D89**, 061704 (2014), arXiv:1310.0378 [hep-ph].
- [39] I. Balitsky and A. V. Grabovsky, “NLO evolution of 3-quark Wilson loop operator,” *JHEP* **01**, 009 (2015), arXiv:1405.0443 [hep-ph].
- [40] Michael Lublinsky and Yair Mulian, “High Energy QCD at NLO: from light-cone wave function to JIMWLK evolution,” *JHEP* **05**, 097 (2017), arXiv:1610.03453 [hep-ph].
- [41] Simon Caron-Huot, “When does the gluon reggeize?” *JHEP* **05**, 093 (2015), arXiv:1309.6521 [hep-th].
- [42] Yuri V. Kovchegov and Heribert Weigert, “Triumvirate of Running Couplings in Small- x Evolution,” *Nucl. Phys.* **A784**, 188–226 (2007), arXiv:hep-ph/0609090 [hep-ph].
- [43] M. A. Braun, “Pomeron with a running coupling in the nucleus,” *Eur. Phys. J.* **C51**, 625–632 (2007), arXiv:hep-ph/0703006 [HEP-PH].
- [44] Fabio Dominguez, A. H. Mueller, Stéphane Munier, and Bo-Wen Xiao, “On the small- x evolution of the color quadrupole and the Weizsäcker-Williams gluon distribution,” *Phys. Lett.* **B705**, 106–111 (2011), arXiv:1108.1752 [hep-ph].
- [45] D. Yu. Ivanov and A. Papa, “The next-to-leading order forward jet vertex in the small-cone approximation,” *JHEP* **05**, 086 (2012), arXiv:1202.1082 [hep-ph].
- [46] This correspondence is a feature of non-global logarithms in jet physics [82]; the latter was identified with BK/JIMWLK evolution by Marchesini and Mueller [83] as well as by Weigert [84], and subsequently significantly developed by Hatta et al. [85–88]. and by Neill [89].
- [47] Alfred H. Mueller, “Conformal spacelike-timelike correspondence in QCD,” *JHEP* **08**, 139 (2018), arXiv:1804.07249 [hep-th].
- [48] This is unlike the case of diffractive DIS [61].
- [49] Since the soft gluon theorem is related to an infinite dimensional Kac-Moody symmetry [90] on the celestial sphere (obtained by a stereographic projection of transverse coordinates) at null infinity, these symmetries may help identify the correct boundary conditions. Note that this theorem is associated with a color memory [91]. In the Regge limit, the latter is precisely the color matrix in Eq. 4 [92] at $x^- = \pm\infty$.
- [50] $p_{J\perp, K\perp}$ are the transverse momenta carried by the two jets and z_J, z_K are their respective momentum fractions relative to the projectile momentum. γ_E is the Euler-Mascheroni constant.
- [51] Jochen Bartels, S. Gieseke, and C. F. Qiao, “The $(\gamma^* \rightarrow q\bar{q})$ Reggeon vertex in next-to-leading order QCD,” *Phys. Rev.* **D63**, 056014 (2001), [Erratum: *Phys. Rev.* **D65**, 079902(2002)], arXiv:hep-ph/0009102 [hep-ph].
- [52] J. Bartels, D. Colferai, S. Gieseke, and A. Kyrieleis, “NLO corrections to the photon impact factor: Combining real and virtual corrections,” *Phys. Rev.* **D66**, 094017 (2002), arXiv:hep-ph/0208130 [hep-ph].

- [53] Jochen Bartels, S. Gieseke, and A. Kyrieleis, “The Process $\gamma^*(L)+q \rightarrow (q\bar{q}g)+q$: Real corrections to the virtual photon impact factor,” *Phys. Rev.* **D65**, 014006 (2002), arXiv:hep-ph/0107152 [hep-ph].
- [54] Ian Balitsky and Giovanni A. Chirilli, “Photon impact factor in the next-to-leading order,” *Phys. Rev.* **D83**, 031502 (2011), arXiv:1009.4729 [hep-ph].
- [55] Ian Balitsky and Giovanni A. Chirilli, “Photon impact factor and k_T -factorization for DIS in the next-to-leading order,” *Phys. Rev.* **D87**, 014013 (2013), arXiv:1207.3844 [hep-ph].
- [56] Guillaume Beuf, “NLO corrections for the dipole factorization of DIS structure functions at low x ,” *Phys. Rev.* **D85**, 034039 (2012), arXiv:1112.4501 [hep-ph].
- [57] Guillaume Beuf, “Dipole factorization for DIS at NLO: Loop correction to the $\gamma_{T,L}^* \rightarrow q\bar{q}$ light-front wave functions,” *Phys. Rev.* **D94**, 054016 (2016), arXiv:1606.00777 [hep-ph].
- [58] Guillaume Beuf, “Dipole factorization for DIS at NLO: Combining the $q\bar{q}$ and $q\bar{q}g$ contributions,” *Phys. Rev.* **D96**, 074033 (2017), arXiv:1708.06557 [hep-ph].
- [59] H. Hanninen, T. Lappi, and R. Paatelainen, “One-loop corrections to light cone wave functions: the dipole picture DIS cross section,” *Annals Phys.* **393**, 358–412 (2018), arXiv:1711.08207 [hep-ph].
- [60] R. Boussarie, A. V. Grabovsky, L. Szymanowski, and S. Wallon, “Impact factor for high-energy two and three jets diffractive production,” *JHEP* **09**, 026 (2014), arXiv:1405.7676 [hep-ph].
- [61] R. Boussarie, A. V. Grabovsky, L. Szymanowski, and S. Wallon, “On the one loop $\gamma^{(*)} \rightarrow q\bar{q}$ impact factor and the exclusive diffractive cross sections for the production of two or three jets,” *JHEP* **11**, 149 (2016), arXiv:1606.00419 [hep-ph].
- [62] R. Boussarie, A. V. Grabovsky, D. Yu. Ivanov, L. Szymanowski, and S. Wallon, “Next-to-Leading Order Computation of Exclusive Diffractive Light Vector Meson Production in a Saturation Framework,” *Phys. Rev. Lett.* **119**, 072002 (2017), arXiv:1612.08026 [hep-ph].
- [63] A. Ayala, M. Hentschinski, J. Jalilian-Marian, and M. E. Tejeda-Yeomans, “Polarized 3 parton production in inclusive DIS at small x ,” *Phys. Lett.* **B761**, 229–233 (2016), arXiv:1604.08526 [hep-ph].
- [64] Giovanni A. Chirilli, Bo-Wen Xiao, and Feng Yuan, “Inclusive Hadron Productions in pA Collisions,” *Phys. Rev.* **D86**, 054005 (2012), arXiv:1203.6139 [hep-ph].
- [65] Giovanni A. Chirilli, Bo-Wen Xiao, and Feng Yuan, “One-loop Factorization for Inclusive Hadron Production in pA Collisions in the Saturation Formalism,” *Phys. Rev. Lett.* **108**, 122301 (2012), arXiv:1112.1061 [hep-ph].
- [66] Anna Stasto, Bo-Wen Xiao, and Feng Yuan, “Back-to-Back Correlations of Di-hadrons in dAu Collisions at RHIC,” *Phys. Lett.* **B716**, 430–434 (2012), arXiv:1109.1817 [hep-ph].
- [67] Tolga Altinoluk, Nestor Armesto, Guillaume Beuf, Alex Kovner, and Michael Lublinsky, “Single-inclusive particle production in proton-nucleus collisions at next-to-leading order in the hybrid formalism,” *Phys. Rev.* **D91**, 094016 (2015), arXiv:1411.2869 [hep-ph].
- [68] B. Ducloué, E. Iancu, A. H. Mueller, G. Soyez, and D. N. Triantafyllopoulos, “Non-linear evolution in QCD at high-energy beyond leading order,” *JHEP* **04**, 081 (2019), arXiv:1902.06637 [hep-ph].
- [69] Zhong-Bo Kang, Yan-Qing Ma, and Raju Venugopalan, “Quarkonium production in high energy proton-nucleus collisions: CGC meets NRQCD,” *JHEP* **01**, 056 (2014), arXiv:1309.7337 [hep-ph].
- [70] Yan-Qing Ma and Raju Venugopalan, “Comprehensive Description of J/Ψ Production in Proton-Proton Collisions at Collider Energies,” *Phys. Rev. Lett.* **113**, 192301 (2014), arXiv:1408.4075 [hep-ph].
- [71] Sanjin Benić, Kenji Fukushima, Oscar Garcia-Montero, and Raju Venugopalan, “Probing gluon saturation with next-to-leading order photon production at central rapidities in proton-nucleus collisions,” *JHEP* **01**, 115 (2017), arXiv:1609.09424 [hep-ph].
- [72] Sanjin Benić and Kenji Fukushima, “Photon from the annihilation process with CGC in the pA collision,” *Nucl. Phys.* **A958**, 1–24 (2017), arXiv:1602.01989 [hep-ph].
- [73] Sanjin Benić, Kenji Fukushima, Oscar Garcia-Montero, and Raju Venugopalan, “Constraining unintegrated gluon distributions from inclusive photon production in proton-proton collisions at the LHC,” (2018), arXiv:1807.03806 [hep-ph].
- [74] Jean Paul Blaizot, Francois Gelis, and Raju Venugopalan, “High-energy pA collisions in the color glass condensate approach. 2. Quark production,” *Nucl. Phys.* **A743**, 57–91 (2004), arXiv:hep-ph/0402257 [hep-ph].
- [75] Fabio Dominguez, Cyrille Marquet, Anna M. Stasto, and Bo-Wen Xiao, “Universality of multiparticle production in QCD at high energies,” *Phys. Rev.* **D87**, 034007 (2013), arXiv:1210.1141 [hep-ph].
- [76] Kevin Dusling, Mark Mace, and Raju Venugopalan, “Parton model description of multiparticle azimuthal correlations in pA collisions,” *Phys. Rev.* **D97**, 016014 (2018), arXiv:1706.06260 [hep-ph].
- [77] Kenji Fukushima and Yoshimasa Hidaka, “General formulae for dipole Wilson line correlators with the Color Glass Condensate,” *JHEP* **11**, 114 (2017), arXiv:1708.03051 [hep-ph].
- [78] I. Balitsky, “Operator expansion for high-energy scattering,” *Nucl. Phys.* **B463**, 99–160 (1996), arXiv:hep-ph/9509348 [hep-ph].
- [79] Yuri V. Kovchegov, “Small x F(2) structure function of a nucleus including multiple pomeron exchanges,” *Phys. Rev.* **D60**, 034008 (1999), arXiv:hep-ph/9901281 [hep-ph].
- [80] E. A. Kuraev, L. N. Lipatov, and Victor S. Fadin, “The Pomernchuk Singularity in Nonabelian Gauge Theories,” *Sov. Phys. JETP* **45**, 199–204 (1977), [*Zh. Eksp. Teor. Fiz.* 72,377(1977)].
- [81] I. I. Balitsky and L. N. Lipatov, “The Pomernchuk Singularity in Quantum Chromodynamics,” *Sov. J. Nucl. Phys.* **28**, 822–829 (1978), [*Yad. Fiz.* 28,1597(1978)].
- [82] A. Banfi, G. Marchesini, and G. Smye, “Away from jet energy flow,” *JHEP* **08**, 006 (2002), arXiv:hep-ph/0206076 [hep-ph].
- [83] G. Marchesini and A. H. Mueller, “BFKL dynamics in jet evolution,” *Phys. Lett.* **B575**, 37–44 (2003), arXiv:hep-ph/0308284 [hep-ph].
- [84] Heribert Weigert, “Nonglobal jet evolution at finite $N(c)$,” *Nucl. Phys.* **B685**, 321–350 (2004), arXiv:hep-ph/0312050 [hep-ph].
- [85] Yoshitaka Hatta, “Relating $e+e-$ annihilation to high energy scattering at weak and strong coupling,” *JHEP* **11**, 057 (2008), arXiv:0810.0889 [hep-ph].
- [86] Emil Avsar, Yoshitaka Hatta, and Toshihiro Matsuo,

- “Soft gluons away from jets: Distribution and correlation,” *JHEP* **06**, 011 (2009), arXiv:0903.4285 [hep-ph].
- [87] Yoshitaka Hatta and Takahiro Ueda, “Resummation of non-global logarithms at finite N_c ,” *Nucl. Phys.* **B874**, 808–820 (2013), arXiv:1304.6930 [hep-ph].
- [88] Y. Hatta, E. Iancu, A. H. Mueller, and D. N. Triantafyllopoulos, “Resumming double non-global logarithms in the evolution of a jet,” *JHEP* **02**, 075 (2018), arXiv:1710.06722 [hep-ph].
- [89] Duff Neill, “The Asymptotic Form of Non-Global Logarithms, Black Disc Saturation, and Gluonic Deserts,” *JHEP* **01**, 109 (2017), arXiv:1610.02031 [hep-ph].
- [90] Temple He, Prahar Mitra, and Andrew Strominger, “2D Kac-Moody Symmetry of 4D Yang-Mills Theory,” *JHEP* **10**, 137 (2016), arXiv:1503.02663 [hep-th].
- [91] Monica Pate, Ana-Maria Raclariu, and Andrew Strominger, “Color Memory: A Yang-Mills Analog of Gravitational Wave Memory,” *Phys. Rev. Lett.* **119**, 261602 (2017), arXiv:1707.08016 [hep-th].
- [92] Adam Ball, Monica Pate, Ana-Maria Raclariu, Andrew Strominger, and Raju Venugopalan, “Measuring color memory in a color glass condensate at electron ion colliders,” *Annals Phys.* **407**, 15–28 (2019), arXiv:1805.12224 [hep-ph].